DV-Xα Study of Electronic Spectra for MoS_4^{2-} and $[(NC)CuS_2MoS_2]^{2-}$ Anions

Qiang Miao,*,†,‡ Hirohiko Adachi,† Isao Tanaka,† and Xin-Quan Xin‡

Department of Material Science and Engineering, Kyoto University, Kyoto 606, Japan, and Department of Chemistry, Nanjing University, Nanjing 210093, China

Received: March 27, 1997; In Final Form: April 25, 1997[⊗]

We have calculated theoretical UV−vis absorption spectra for tetrahedral MoS_4^{2-} and $[(NC)CuS_2MoS_2]^{2-}$ anions by the use of DV-Xα cluster method. The calculated spectra for both anions are in good agreement with the experiments. The results show that the first and the second band in the spectra for both anions are principally caused by the electronic transitions within the MoS_4 core, relating to the HOMO $1t_1$ and LUMOs 2e and $3t_2$. The third band is sensitively affected by the structure of MoS_4 core and its environment. In the case of simple MoS_4^{2-} anion, the third band not only shifts by the Mo−S bond length but also is expected to change the structure by its environment. The third band of $[(NC)CuS_2MoS_2]^{2-}$ is changed by the interaction among Cu 3d, Mo 4d, and S 3p orbitals. We have also tried to clarify the real structure of MoS_4^{2-} anion in the actual solution, by calculating various clusters with different Mo−S distances, and have found the cluster with the bond length of 2.22Å provided the best fit to the experimental spectrum.

I. Introduction

The thiomolybdates MoS_4^{2-} and their derivative $[(NC)CuS_2MoS_2]^{2-}$ anions are of interest, not only from a standpoint of structural chemistry but also from better understanding of the chemical basis for the interpretation of Cu−Mo−S interactions in biological systems.[1−3] Therefore, a reliable theoretical study on the electronic structure is very important for interpretation of various experimental results such as the UV−vis absorption spectrum. However, only the MoS_4^{2-} anion has been calculated by means of the first-principles method probably because of its large-scale calculation even for simple clusters.

The visible and the near UV region absorption spectra of both compounds have experimentally been measured and discussed.[1−2] Müller et al.[1] have found, from comparison of the spectra between the two species, MoS_4^{2-} and $[(NC)CuS_2MoS_2]^{2-}$ in acetonitrile, the first and the third of the three longest wavelength bands are changed in their structure by complex formation, while the second band is essentially unaltered in its position, intensity, and half-width. Gheller et al.[2] further pointed out that the first region is split into at least two bands due to the raising of the degeneracy of the t_1 level in the lower symmetry of the complex.

The semiempirical EH-SCCC-MO calculations,[4] the SW-Xα methods.[5,6] the local density pseudopotential method,[7] and the symmetry-adapted cluster expansion methods[8] have been reported for the tetrathiomolybdate MoS_4^{2-} cluster. So far, only semiempirical methods have been used on Cu−Mo−S clusters. Müller et al. have pointed out by using semiempirical MO calculation results[1] that on complex formation the t_1 orbitals of MoS_4^{2-} ligands are much more strongly disturbed than $3t_2$, 2e, and $4t_2$ MOs, and the t_1 orbital is not involved in the second band.

In comparing the calculated spectrum with the experiment in solution conditions, one should notice the effect of structural modifications. That is, we usually lack accurate information on the real state of molecular structure in the actual experimental condition. Therefore, we cannot obtain the very accurate theoretical results even for the very simple situation of MoS_4^{2-}. In general, the strong and long-range electrical interaction between ions may raise a very high inner pressure by a crystal packing. The high pressure can lead to a shortening of bond lengths and to a distortion of molecular structure from higher symmetry. This may cause split energy levels and a shift of spectral peaks. One of the most realistic ways to obtain information on the real structure is to perform the model cluster calculation varying its structure and to find the most proper structure that gives the best fit for the experimental spectrum.

In the present paper, we first calculate the electronic states of MoS_4^{2-} and $[(NC)CuS_2MoS_2]^{2-}$ clusters, by the use of the DV-Xα molecular orbital method[9] and compare our calculated results with the previous studies as well as the experimental spectrum for MoS_4^{2-}. Next we perform the cluster calculation to understand the electronic spectrum of $[(NC)CuS_2MoS_2]^{2-}$. We theoretically examine the absorption bands especially in the region of 2−6 eV. For the theoretical spectrum, the peak energy is evaluated by the level separation between the initial and final states in the electronic transition obtained from Slater's transition state calculation. The peak intensity is estimated by the first-principles calculation of the dipole transition probability. We also attempt to find a proper Mo−S bond length for the MoS_4^{2-} anion in acetonitrile by comparing the theoretical spectrum with experiment. Furthermore, the reasons for the split in the first band and the peak shoulder of the third band have been studied in detail.

II. Computational Method

The MoS_4^{2-} anion consists of a central molybdenum atom surrounded tetrahedrally by four sulfur atoms at 2.177 Å[10] in the solid state. The molecular geometry of the $[(NC)CuS_2MoS_2]^{2-}$ anion, as a crystallographically independent unit, is taken from the experimental data of $(n\text{-}Pr_4N)_2[(NC)CuS_2MoS_2]$.[2] This aggregate approximates to C_{2v} symmetry, in which the molybdenum atom sits at the center of the essentially tetrahedral MoS_4 unit. The mean values of Mo−S(bridging) and Mo−S(terminal) bond lengths are 2.2255 and 2.150 Å, respectively. The bond angles are taken to be 106.6° and 110.4° for the S(bridging)−Mo−S(bridging) and S(terminal)−Mo−S(termi-

* All correspondence should be addressed to Qiang Miao, Department of Chemistry, Nanjing University, Nanjing 210093, P.R. of China. FAX: (86)-25-3317761.
† Kyoto University.
‡ Nanjing University.
⊗ Abstract published in *Advance ACS Abstracts,* July 1, 1997.

S1089-5639(97)01097-9 CCC: $14.00

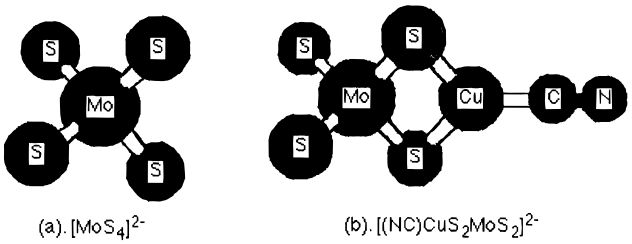

Figure 1. Perspective view of model clusters for (a) the tetrahedral MoS_4^{2-} and (b) the $[(NC)CuS_2MoS_2]^{2-}$ anions.

nal), respectively. The triangular coordinated copper atom is bound to the MoS_4 core across the S(bridging)−S(bridging) edge with a mean Cu−S(bridging) bond length of 2.217 Å. We show a perspective view of the two anion clusters in Figure 1.

The details of the computational DV-Xα method have thoroughly been described in elsewhere.[9] In the present calculations, the exchange scaling parameter α in Slater's exchange potential[12] was taken to be 0.70 for all atoms and both compounds. In the present version of the DV-Xα program we used, numerical basis functions can flexibly be changed according to the electron configuration of atoms in molecule. The main advantage of the use of the numerical basis is reduction of basis set, so that a small size numerical basis can provide highly accurate wave functions for molecules and clusters. The numerical atomic orbitals, in the present work, including Mo 1s−5p, Cu 1s−4p, S 1s−3p, C 1s−2p, and N 1s−2p are employed as the basis functions.

In the finite field method, stationary perturbation theory provides an evaluation of the probability for vertical excitation by the use of oscillator strength. Within the one-electron model dipole approximation and expressed in the length form, the oscillation strength of a transition between an initial state $|\psi_i\rangle$ and a final state $|\psi_f\rangle$ is given by[15]

$$f_{\alpha,(i\rightarrow f)} = (2/3)\omega_{if}|\langle\psi_i|\mathbf{r}_\alpha|\psi_f\rangle|^2 \qquad (1)$$

where ω_{if} is the excitation energy, and α is the direction in which the external field is applied. Within the DV-Xα framework, we make the first-principles calculation for the dipole transition matrix including the crossover transitions.[13] By applying the field in different directions, it is possible to obtain the different components of the dipole transition probability f_α. In the case of a homogeneous solution, the total probability should be averaged $f_{\alpha,(i\rightarrow f)}$ in three directions:

$$f_{(i\rightarrow f)} = (1/3)\sum_\alpha f_{\alpha,(i\rightarrow f)}$$

A description of the dipole transition in different directions is unnecessary for a higher symmetrical cluster. However, it is helpful in explaining the differences and relations of spectral phenomena for molecules with different symmetries.

The peak intensities of theoretical spectra are obtained by a assuming a Gaussian distribution as

$$I(\omega) = \sum_{i,f} f_{(i\rightarrow f)}/(2\pi)^{1/2}\sigma \exp[-(\omega-\omega_{if})^2/2\sigma^2]$$

The peak width σ, in the present work, is determined in an arbitrary way but the same for each peak.

In the DV-Xα method, an accurate transition energy could be estimated as the energy separation between the two levels from a calculation of Slater's transition state[14] in which both the initial and final states hold one half electron:

$$\omega_{if} = \omega_f - \omega_i$$

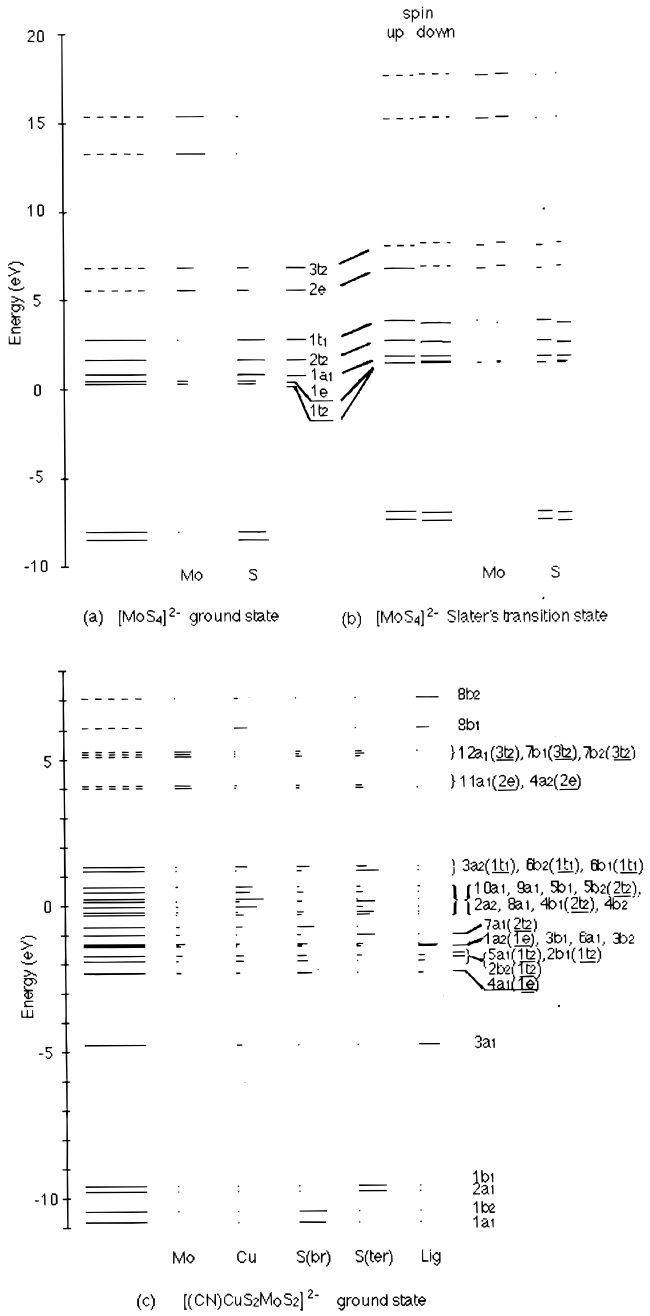

Figure 2. Energy levels and atomic components for (a) MoS_4^{2-} in the ground state, (b) in Slater's transition state, and (c) $[(NC)CuS_2MoS_2]^{2-}$ in the ground state. The br denotes bridging, ter terminal, and Lig ligand.

The Slater's transition state is halfway excited between the initial and the final state, so the effects of the orbital relaxation and reconstruction in the process have been included. It is expected that the dipole transition probability of eq 1 is more accurately computed by using the wave function of the transition state than those of the ground state or excited state.

III. Results and Discussions

1. Electronic States of $[MoS_4]^{2-}$ and $[(CN)CuS_2MoS_2]^{2-}$ Anions. Figure 2a,c illustrates the valence state energy levels of ground states for $[MoS_4]^{2-}$ and $[(CN)CuS_2MoS_2]^{2-}$ clusters shown in Figure 1. The atomic components obtained from Mulliken's population analysis are also demonstrated in the figure. The Mulliken's atomic valence orbital populations in the clusters are displayed in Table 1. In the present paper, we will focus on the general characteristics of the valence electronic state in order to understand the experimental absorption spectra.

TABLE 1: Mulliken Atomic Valence Orbital Populations in the Clusters[a]

		1	2
Mo	4d	4.081	4.258
	5s	0.055	0.090
	5p	0.299	0.287
Cu	3d		9.598
	4s		0.457
	4p		0.477
S_{term}	3s	1.965	1.967
	3p	4.923	4.788
S_{μ}	3s		1.955
	3p		4.781

[a] **1** and **2** stand for $[MoS_4]^{2-}$ and $[(NC)CuS_2MoS_2]^{2-}$ clusters, respectively.

The valence state of the $[MoS_4]^{2-}$ cluster mainly consists of S 3p orbitals with an admixture of some amounts of Mo 4d. Above the S 3p band, unoccupied Mo 4d levels with a considerable large amount of S 3p components are located. The electronic configuration of the ground state in the valence state region of $[MoS_4]^{2-}$ is $(1t_2)^6(1e)^4(1a_1)^2(2t_2)^6(1t_1)^6$. By the formation of an S_4 tetrahedron cage, the S 3s orbitals split into the lowest two levels, a_1 and t_2 admixed with very small components of Mo 5s in a_1 and 4d in t_2. These levels are rather strongly localized and have neither essential contribution to Mo−S nor S−S bonding in the molecule. The S 3p orbitals split into a_1, e, t_1, and two t_2 levels, and Mo 4d orbitals split into an e and t_2 levels, respectively. The significant interactions between the two e orbitals, and between the two t_2 orbitals produce 1e π-bonding and $1t_2$ σ-bonding levels, and their antibonding partners 2e and $3t_2$ as LUMOs, respectively. The $1a_1$ has a weak antibonding character of S 3p with small amounts of Mo 5s and S 3s. The remaining two filled levels $2t_2$ and $1t_1$ are mainly constructed by S 3p, and the $2t_2$ is slightly bonding while $1t_1$, the HOMO, nonbonding. The LUMOs are 2e and $3t_2$, and 2e is located at 2.81 eV above the HOMO $1t_1$. Most of the Mo 4d components are contained in these 2e and $3t_2$ MOs. Finally, the two highest unoccupied levels, $2a_1$ and $4t_2$, are mainly composed of Mo 5s and Mo 5p, respectively, and located at about 10 eV higher than the HOMO.

The ground state energy level diagram for $[(CN)CuS_2MoS_2]^{2-}$ is displayed in Figure 2c. The $[(CN)CuS_2MoS_2]^{2-}$ anion has 25 occupied Cu−S−Mo levels in the valence state region. The manifold HOMOs $\underline{1t_1}$ are substantially composed of $1t_1$ MOs of the $[MoS_4]^{2-}$ cluster. LUMOs $\underline{2e}$ and $\underline{3t_2}$ mainly come from 2e and $3t_2$ of $[MoS_4]^{2-}$, respectively, and almost keep their level structure, with splits less than 0.2 eV and not being explicitly affected by the bounding of the Cu atom. In this cluster, there are four S atoms, two of which are nonbridging (terminal) and other two are bridging between Mo and Cu atoms. The four S 3s orbitals split into two lower bridging, a_1 and b_2, and into two others of terminal, a_1 and b_1, lying lowest in valence state. By the bridge bonding with the Cu atom, the bridging S 3p orbitals of the MoS_4 group tend to primarily contribute to $\underline{1t_2}$ and interact with both Mo 4d and Cu 3d, forming a delocalized multicenter bond over the Cu−(μ−S)$_2$−Mo network. The terminal S 3p orbitals contribute to make a rather localized $\underline{2t_2}$ MO with a small component of Mo 4d. The principal components of Mo 4d are still found in the LUMOs $\underline{2e}$ and $\underline{3t_2}$, which are essentially constructed by the 2e and $3t_2$ of the MoS_4 cluster. Most of the Cu 3d except for d_{z^2} is not largely involved in the bonding levels. It forms levels near 0 eV. A small component of Cu 4p is found in the occupied levels, and a slight contribution of Cu $3d_{z^2}$ is found in the second lowest unoccupied level $a_1(\underline{2e})$.

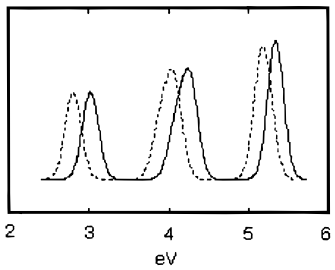

Figure 3. Comparison of theoretical spectra of the MoS_4^{2-} cluster calculated from Slater's transition state (solid line) with that from the ground state (dotted line).

2. Theoretical Calculation of Absorption Spectra. The experimental UV−vis absorption spectra for $(NMe_4)_2MoS_4$ and $(NMe_4)_2[(CN)CuS_2MoS_2]$ show three peaks in the energy range 2−6 eV. These are considered to be due to charge transfer transitions. As mentioned above, we perform the first-principles calculation of the absorption spectrum within the DV-Xα framework. In general, the difference in energy levels between two spin orbitals or/and the change of spin state in a transition metal system may be caused in the transition process. In the present case with the main Mo(4d) component in the LUMO of the Mo(d^0) systems, the difference in the two spin levels is not obviously large (see Figure 2b) so that the low spin state could approximately be used in the theoretical spectrum estimation for the title clusters to save expensive computing time. Since the transition energy and peak's intensity could be obtained from either Slater's transition state or the ground state, the sensitivity of the numerical results is checked by comparison of theoretical spectra of the two calculation methods for MoS_4^{2-} displayed in Figure 3. The difference in peak energies resulting from the ground state and the Slater's transition state calculations is about 0.2 eV, but the peak intensities are almost same. In the following, for reasons we just discussed, the peak energies are evaluated by the energy separation between relevant levels of Slater's transition state; namely, the initial and final states in the electronic transition and the peak intensity are estimated by the calculation of the dipole transition probability. Figure 4 demonstrates the comparison of the theoretical and experimental absorption spectra for MoS_4^{2-} and $[(CN)CuS_2MoS_2]^{2-}$. We calculate for the model clusters mentioned above. The theoretical spectra show, in general, fairly good agreement with experiments except a discrepancy of peak energies of 0.2−0.4 eV for MoS_4^{2-}.

A. $[MoS_4]^{2-}$. For MoS_4^{2-}, some calculations for the absorption spectra have been reported by other workers.[4−8] Table 2 summarizes the theoretical results of the present and previous studies as well as the experimental data for $(NMe_4)_2MoS_4$ in acetonitrile. As seen in Figure 4a, the optical absorption bands of the MoS_4^{2-} anion are broadened from 2 to 6 eV, in which three principal peaks are involved at about 2.65, 3.91, and 5.12 eV, respectively. From the valence state levels calculated, we expect the MOs $1t_2$, 1e, $1a_1$, $2t_2$, and $1t_1$ as the initial states and the 2e and $3t_2$ as the final states participate in these transitions. We have calculated eight allowed and two forbidden dipole transitions.

The lowest allowed transition at 2.65 eV, accompanying an electron transfer from the ligand nonbonding S 3p level to the antibonding Mo 4d level, is assigned as $1t_1$(S 3p) → 2e(MO with interaction of Mo 4d−S 3p). This is a transition from HOMO to LUMO. Our assignment is the same as most of the previous studies. The calculated transition energy is very close to that of SAC−CI theory[8] (3.02 vs 3.03 eV), although slightly larger than the experimental values.

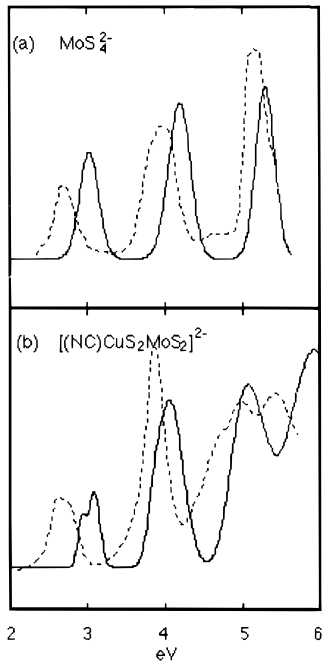

Figure 4. Electronic absorption spectra of MoS_4^{2-} and $[(NC)CuS_2MoS_2]^{2-}$ anions. Solid lines stand for the theoretical and dotted lines for the experiments of $(NMe_4)_2MoS_4$ (digitized after ref 11) and $(NMe_4)_2[(NC)CuS_2MoS_2]$ (digitized after ref 1) in acetonitrile.

The second band from 3.5 to 4.5 eV, shown in Figure 4a, seems to include more than one transition in this energy range. The present calculation suggests $2t_2$(S 3p) → 2e(Mo 4d−S 3p) for the lower and $1t_1$(S 3p) → $3t_2$(Mo 4d−S 3p) for the higher energy transition. The intensity and half-width of this peak should be determined by the separation and strengths of the two peaks. The present result for $1t_1 \rightarrow 3t_2$ shows a very good correspondence to experiment, although the peak energy, 4.23 eV, is about 0.32 eV higher. The weaker transition of $2t_2 \rightarrow$ 2e with the oscillator strength of 0.104 seems to be in good agreement with that of the higher one by SAC−CI calculation,[8] but this may correspond with the shoulder of about 3.6 eV seen in the experimental spectrum. The present transition probability of 0.128 for the peak at 4.23 eV is closer to the experimental data than that given by SAC−CI theory.[8]

The third band from 4.7 to 5.4 eV seems to be similar to the second band. It consists of two very closed allowed transitions $1t_2 \rightarrow$ 2e and $2t_2 \rightarrow 3t_2$. Since the $2t_2$ orbital in the ground state has smaller Mo 4d components than $1t_2$ does, it can be expected that the second transition of the charge transfer has a large probability. Our calculation suggests this by giving a considerably large oscillator strength of 0.101.

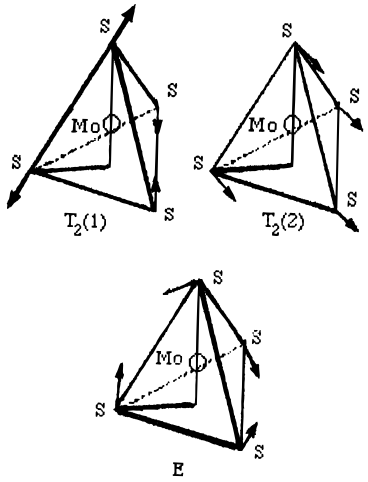

Figure 5. Assumed molecular distortion modes from T_d symmetry.

As seen in the experimental spectrum, there is also a weak shoulder about 4.62 eV below the third peak. This shoulder peak can be considered as being due to the dipole-forbidden transition, which is allowed through molecular vibration. Our calculation indicates that this peak is assigned to $1a_1$(S 3p) → 2e(Mo 4d−S 3p). In order to confirm it, we assume that the cluster model distorted during thermal vibrations by moving out sulfur atoms 2.0% of its bond length from T_d symmetry (see Figure 5). The correspondent transition energies of $1a_1 \rightarrow$ 2e in the vibration modes of $T_2(1)$, $T_2(2)$, and E are distributed from 4.84 to 5.06 eV, and the oscillator strengths are calculated to be approximately 0.4×10^{-2}. Although it is difficult to simulate all the vibration modes with exact amplitude and the present calculation of oscillator strength could not quantitatively correspond with the experiment, it is possible to assign the shoulder to the transition of $1a_1 \rightarrow$ 2e.

In order to clarify a realistic structure of the MoS_4^{2-} anion existing in the actual solution, several assumptions for the Mo−S bond length are made and the cluster calculations are performed so as to give a theoretical spectrum that coincides with the experiment. We find the theoretical spectrum for the model cluster with a Mo−S bond of 2.22 Å shows good agreement with the experiment, as shown in Figure 6. The peak energies and intensities for the first and second peaks almost completely fit the experiment, while the intensity of the third peak is not satisfactory. This discrepancy may be due to a solution effect. That is, the third band of the spectrum of the MoS_4^{2-} cluster is sensitively affected by its outer spherical coordination. This is further confirmed by $[(CN)CuS_2MoS_2]^{2-}$ spectrum calculations (see text below). The states concerning the first and second peaks are the frontier orbitals as discussed above. However,

TABLE 2: Assignments of the Optical Excitations, the Calculated Transition Energies ν_i (eV), and Oscillator Strengths in MoS_4^{2-}

	first band			second band			third band		
	ν_1	f_1^i	assign.[a]	ν_2	f_2^i	assign.[a]	ν_3	f_3^i	assign.[a]
expt[c]	2.65	0.1		3.91	0.2		5.12	0.32	
present work	3.02	0.241	$1t_1 \rightarrow$ 2e	4.09	0.104	$2t_2 \rightarrow$ 2e	5.29	0.070	$1t_2 \rightarrow$ 2e
				4.23	0.128	$1t_1 \rightarrow 3t_2$	5.30	0.101	$2t_2 \rightarrow 3t_2$
SCCC[d]	3.20		$1t_1 \rightarrow$ 2e	4.20		$1t_1 \rightarrow 3t_2$	4.90		$2t_2 \rightarrow$ 2e
SW-Xα[e]	1.90		$1t_1 \rightarrow$ 2e	3.50		$1t_1 \rightarrow 3t_2$	3.89		$1t_2 \rightarrow$ 2e
	2.50		$2t_2 \rightarrow$ 2e	4.20		$2t_2 \rightarrow 3t_2$	4.80		$1a_1 \rightarrow$ 2e
SW-Xα[f]	2.7		$2t_2 \rightarrow$ 2e	3.4		$1t_1 \rightarrow 3t_2$	5.5		$1e \rightarrow 3t_2$
LDT[g]	2.50		$1t_1 \rightarrow$ 2e	3.50		$2t_2 \rightarrow$ 2e	4.90		$2t_2 \rightarrow 3t_2$
				3.89		$1t_1 \rightarrow 3t_2$			
SAC-CI[h]	3.03	0.157	$1t_1 \rightarrow$ 2e	3.83	0.037	$1t_1 \rightarrow 3t_2$	5.20	0.0004	[b] $2t_2 \rightarrow 3t_2$
				4.34	0.095	$2t_2 \rightarrow$ 2e	5.65	0.264	[b] $1t_1 \rightarrow 3t_2$

[a] Indicated relative to the HF configuration in Figure 2a. [b] With mixed configurations. [c] Reference 11. [d] Reference 4. [e] Reference 5. [f] Reference 6. [g] Reference 7. [h] Reference 8. [i] Average oscillator strength.

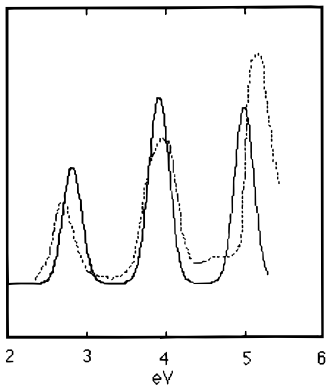

Figure 6. Comparison of the calculated spectrum of MoS_4^{2-} with a Mo−S distance of 2.22 Å (solid line) with experiment (dotted line).

the third peak is ascribed to the transitions from Mo 4d−S 3p bonding levels to the antibonding Mo 4d levels. In an actual solution, solvent molecules can sensitively affect the AO compositions of the Mo−S bonding, although in the present calculation we take only the simple model cluster MoS_4^{2-}; thus the effects of the solvent molecules in the environment are not taken into account. Thus, if the Mo−S bond length of MoS_4^{2-} in real solution is concerned, only the first two theoretical spectral bands are needed to meet with those of the experiment. From the comparison between the calculated and experimental spectra, the Mo−S bond length for MoS_4^{2-} in acetonitrile solution can be expected to be 2.22 Å, which is somewhat longer than the value 2.177 Å for the first cluster model taken from the experimental data of the solid state. This implies that an inner pressure acting on the MoS_4^{2-} cluster is stronger in a solid than that in the acetonitrile liquid solution.

B. [(CN)CuS₂MoS₂]²⁻. Since the $[(CN)CuS_2MoS_2]^{2-}$ anion contains an MoS_4 unit in its structural center, an electronic structure similar to that of the MoS_4^{2-} cluster can be expected. As shown in Figure 2c, the $\underline{1t_1}$, $\underline{2e}$ and $\underline{3t_2}$ as the highest occupied and the lowest unoccupied MoS_4 group's orbitals are somewhat split but are not seriously disturbed by bonding of the copper atom.

The electronic spectrum is broadened in the range from 2 to 6 eV similar to the case of $[MoS_4]^{2-}$. Within this energy range, about 20 molecular orbitals are included in the initial states and seven in final states for the transitions. Totally, about 92 allowed and forbidden transitions have been calculated to provide the theoretical spectrum. The calculated transition energies and their orbital characteristics are listed in Table 3.

From Figure 4b, one can find that the lowest band of the theoretical spectrum is split into two peaks. The present calculations indicate that all five initial states involved in the region are from $\underline{1t_1}$ fragments and two final states are $\underline{2e}$ fragments of MoS_4. This is a situation similar to the case of the simple MoS_4^{2-} anion. The first peak in this band region with the calculated energy 2.93 eV resulted from a transition of HOMO($a_2(\underline{1t_1})$) → LUMO($a_2(\underline{2e})$). Although the Cu 3d orbital participates in the $a_2(\underline{1t_1})$, it is found from the Mulliken population analysis that the charge transfer substantially takes place from the bridging sulfur to molybdenum atom during this transition. The second peak contains four transitions. Two of them are assigned to the transitions from $b_2(\underline{1t_1})$ to $a_2(\underline{2e})$ and $a_1(\underline{2e})$ accompanied by an electron transfer LCu → Mo−S(terminal), where L denotes the ligand CN. The other two are from $b_1(\underline{1t_1})$ to a_2 and a_1 with charge transfer S(terminal) → Mo. The different types of charge transfers take place; then the splitting of the band is caused not only by reduction of symmetry but also by admixture with Cu 3d into $\underline{1t_1}$. The peak separation of about 0.15 eV reflects the LCu−MoS_4 weak interactions at these levels.

As pointed out by Müller, the second band is almost unchanged in peak energy, intensity, and half-width compared with that of simple MoS_4^{2-}. According to the present calculations, there are about 12 dipole-allowed transitions in this band range. Among the 12 allowed transitions, six are originating from $\underline{1t_1}$ → $\underline{3t_2}$, similar to that of the simple MoS_4^{2-} anion, since the $\underline{1t_1}$ and $\underline{3t_2}$ levels are not seriously reorganized by bonding of the copper atom. However, the donors and acceptors during the transitions are somewhat different from simple the MoS_4^{2-} anion. In the case of MoS_4^{2-}, the second band was caused by the charge transfer from $2t_2$(S 3p) to 2e(Mo 4d−S 3p antibonding), while in the $[(CN)CuS_2MoS_2]^{2-}$ several processes, namely, several transitions of S(terminal) → Mo, S(bridging)−S(terminal) → Mo, LCu−S(bridging) → Mo, LCu → Mo, and S(bridging) → Cu−Mo, are included. Two transitions in this band are assigned as $b_2(\underline{2t_2})$ → $\underline{2e}$, which show energies similar to that of the MoS_4^{2-} anion, accompanied by the electron transfer of S(terminal) → Mo−S(bridging). Four other states of $\underline{2t_2}$ → $\underline{2e}$ shift to the next band region due to rather strong Cu−MoS_4 interaction in these MOs. The remaining four allowed transitions in this band are assigned to those

TABLE 3: Transition Energies Δ*E* (eV) and Orbital Characteristics of the $[(CN)CuS_2MoS_2]^{2-}$ Model Cluster

	$4a_2(\underline{2e})$	$11a_1(\underline{2e})$	$7b_2(\underline{3t_2})$	$7b_1(\underline{3t_2})$	$12a_1(\underline{3t_2})$	$8b_1$	$8b_2$
$3a_2(\underline{1t_1})$	2.933	2.941*	3.941	3.981	4.104*	5.542	7.275
$6b_2(\underline{1t_1})$	3.120	3.078	4.112	4.140*	4.282	5.346*	6.836
$6b_1(\underline{1t_1})$	3.040	3.098	4.083*	4.098	4.228	5.713	7.219*
$10a_1$	3.917* [a]	3.861	4.929	4.941	5.084	5.969	
$9a_1$	4.300*	4.294	5.338	5.356	5.483	6.810	
$5b_1$	3.990	3.956	4.985*	5.017	5.155	6.172	
$5b_2(\underline{2t_2})$	4.078	4.125	5.121	5.183*	5.266	6.730*	
$2a_2$	4.769	4.710*	5.798	5.839	5.949*		
$8a_1$	4.956*	4.887	5.988	5.989	6.130		
$4b_1(\underline{2t_2})$	4.804	4.728	5.829*	5.844	5.980		
$4b_2$	5.070	5.043	6.050	6.128*	6.247		
$7a_1(\underline{2t_2})$	5.140*	5.208	6.202	6.220	6.347		
$1a_2(\underline{1e})$	5.496*	5.469	6.485				
$3b_2$	6.026	5.926	6.960				
$6a_1$	5.797*	5.766	6.765				
$3b_1$	5.695	5.712	6.714*				
$2b_1(\underline{1t_2})$	8.249	8.127	8.477				
$5a_1(\underline{1t_2})$	6.450*	6.369					
$2b_2(\underline{1t_2})$	8.269	8.146	8.510				
$4a_1(\underline{1e})$	8.340*	8.213					

[a] The asterisk indicates a dipole−dipole forbidden transition.

from localized Cu 3d orbitals to 2e. During these transitions, molecular orbitals with interactions of S(bridging)−S(terminal), Mo−S(bridging), and Mo−S(terminal) are the acceptors, respectively.

The third band, which contains two strong peaks, as seen in Figure 4b, is totally different from that of the simple MoS_4^{2-} anion due to strong interactions between Cu 3d and Mo 4d−S 3p bonding. Most of the transitions originating from the MoS_4 core are not so important in the present case since their oscillator strengths are very small. The first peak of this band is constructed by three principal transitions of $Cu(d_{z^2}) \rightarrow 3t_2$. Thus Mo and bridging S atoms obtain electron charge during the transition. The second peak involves four stronger transitions. Two of them are assigned as S(bridging)−S(terminal) → Mo−Cu(p), while other two LCu → Mo−S(bridging). The transition properties of the band and the practical band change of the spectrum of the cluster from that of the MoS_4^{2-} are other evidence that the third band of the electronic absorption spectrum of MoS_4^{2-} is sensitively affected by its outer spherical atomic or moleculer coordinating discussed above.

IV. Conclusion

We have calculated the electronic states and theoretical spectra for the tetrahedral MoS_4^{2-} anion and $[(NC)CuS_2MoS_2]^{2-}$. The calculated spectra are in good agreement with experiment.

The results show that the first and the second band in the spectra for both anions are principally determined by the electronic transitions within the MoS_4 core, namely, the HOMO $1t_1$ and LUMOs 2e and $3t_2$. The peak energies are considerably affected by the Mo−S bond length. In order to find the real structure of the MoS_4^{2-} anion in solution, we have tried to calculate the theoretical spectrum varying the Mo−S bond length and found the cluster with a bond length of 2.22 Å provided the best fit of the first two bands to experiment. Since the electronic state of the MoS_4 core does not largely vary in bonding of the copper atom, the lowest two bands almost keep their structures in the $[(NC)CuS_2MoS_2]^{2-}$ spectrum, when compared with that of MoS_4^{2-}.

As mentioned above, in the case of the simple MoS_4^{2-} anion, the peak energy of the third band also shifts by the Mo−S bond length. Furthermore, the present calculation implies that the third band is sensitively affected by the environment of MoS_4. The third band of $[(NC)CuS_2MoS_2]^{2-}$ is also changed by the interaction among Cu 3d, Mo 4d, and S 3p orbitals. Chemically, by theoretical and experimental studies of the third band of the electronic absorption spectrum of the MoS_4-containing cluster, one could obtain information on the interaction of the MoS_4 core with its outer spherical atoms or molecules.

References and Notes

(1) Müller, A.; Diemann, E.; Jostes, R.; Bögge, H. *Angew. Chem., Int. Ed. Engl.* **1981**, *20*, 934.
(2) Gheller, S. F.; et al. *Inorg. Chem.* **1984**, *23*, 2519.
(3) Jeannin, Y.; Sécheresse, F.; Bernès, S.; Robert, F. *Inorg. Chim. Acta* **1992**, *198*−*200*, 493.
(4) Kebabcioglu, R.; Müller, A. *Chem. Phys. Lett.* **1971**, *8*, 59.
(5) Onopko, D. E.; Titov, S. A. *Opt. Spectrosc. (Engl. Transl.)* **1979**, *47*, 185.
(6) Kutzler, F. W.; Natoli, C. R.; Misemer, D. K.; Doniach, S.; Hodgson, K. O. *J. Chem. Phys.* **1980**, *73*, 3274.
(7) Bernholc, J.; Stiefel, E. I. *Inorg. Chem.* **1985**, *24*, 1323.
(8) Nakatsuji, H.; Saito, S. *J. Chem. Phys.* **1990**, *93*, 1865.
(9) Adachi, H.; Tsukada, M.; Satoko, C. *J. Phys. Soc. Jpn.* **1978**, *45*, 875. The DV−Xα method was first developed for band structure calculation (Ellis, D. E.; Painter, G. S. *Phys. Rev.* **1970**, *B2*, 2887) and then used for cluster calculations (Baerends, E. J.; Ellis, D. E.; Ros, P. *Chem. Phys.* **1973**, *2*, 41; Ellis, D. E.; Adachi, H.; Averill, F. W. *Surf. Sci.* **1976**, *58*, 497). The way to generate numerical basis functions and some other points are modified in the present version of the DV−Xα program. The details of this program are described in ref 9.
(10) Clegg, W.; Garner, C. D.; Nicholson, J. R. *Acta Crystallogr., Sect. C* **1983**, *39*, 552
(11) Müller, A.; Diemann, E. *Chem. Phys. Lett.* **1971**, *9*, 369.
(12) Slater, J. C. *Phys. Rev.* **1951**, *81*, 385; **1951**, *82*, 538.
(13) Adachi, H.; Taniguchi, K. *J. Phys. Soc. Jpn.* **1980**, *49*, 1944.
(14) Slater, J. C. *Quantum Theory of Molecules and Solids*; McGraw-Hill: New York, 1974; Vol. 4, p 51.
(15) Craig, D. P.; Thirunamachandran, T. *Molecular Quantum Electrodynamics*; Academic: New York, 1984.